

# ESTIMATION OF DISSOLUTION RATE FROM IN-VIVO STUDIES OF SYNTHETIC VITREOUS FIBERS

*Walter Eastes, Russell M. Potter, and John G. Hadley*

Owens Corning, Science and Technology Center, Granville, Ohio, USA

Originally published:  
*Inhalation Toxicology*, in press (2000)

Copyright © 2000 Taylor & Francis

## ABSTRACT

Although the dissolution rate of a fiber was originally defined by a measurement of dissolution in simulated lung fluid in vitro, it is feasible to determine it from animal studies as well. The dissolution rate constant for a fiber may be extracted from the decrease in long fiber diameter observed in certain intratracheal instillation experiments or from the observed long fiber retention in short-term biopersistence studies. These in-vivo dissolution rates agree well with those measured in vitro for the same fibers. For those special types of fibers, the high-alumina rock wool fibers that could not be measured in vitro, the method provides a way of obtaining a chemical dissolution rate constant from an animal study. The inverse of the in-vivo dissolution rate, the fiber dissolution time, correlates well with the weighted half life of long fibers in a biopersistence study, and the in-vivo dissolution rate may be estimated accurately from this weighted half life.

## INTRODUCTION

The dissolution rate constant  $k_{dis}$  of a fiber is a quantity most often determined from the measurement of fiber dissolution in simulated lung fluid in vitro ([Scholze, 1988](#)). It has been shown also, however, that the dissolution rate constant may be used to predict the rate of decrease in fiber diameter after intratracheal instillation in rats ([Eastes et al., 1995](#)), the biopersistence of long fibers after short-term inhalation ([Bernstein et al., 1996](#); [Eastes and Hadley, 1995](#)), and the incidence of fibrosis and lung tumors after chronic inhalation and tumors following intraperitoneal injection in rats ([Hesterberg et al., 1998](#); [Eastes and Hadley, 1996](#); [Eastes and Hadley, 1994](#)). The ability of the in-vitro measured dissolution rate constant to predict the behavior of long fibers in vivo implies therefore that  $k_{dis}$  could be estimated directly from the results of a biopersistence study. This paper describes a method for obtaining an "in-vivo dissolution rate constant" from the measurement of long fiber retention following short-term inhalation and from intratracheal instillation studies that produce the requisite fiber diameter data.

The ability to determine such an in-vivo dissolution rate is useful for at least two reasons: First, it enables a dissolution rate to be obtained for fiber types that cannot yet be measured accurately by the existing in-vitro protocol, if biopersistence studies of such fibers have been carried out. One class of fibers for which in-vitro measurements are presently inadequate, and for which a number of biopersistence studies have been reported, are the high-alumina content rock wool fibers ([Knudsen et al., 1996](#)). This paper derives in-vivo dissolution rate constants for a series of these types of fibers, which may be used to elucidate the dependence of  $k_{dis}$  on composition for these fibers in a manner similar to that previously published for borosilicate glass wool fiber compositions ([Eastes et al., 2000](#)), which was based on in-vitro dissolution ([Mattson, 1994](#); [Potter and Mattson, 1991](#)). Second, it allows researchers to compare in-vivo dissolution with that measured in vitro in terms of a chemical reaction parameter  $k_{dis}$  to determine where improvements need to be made in the in-vitro methods to better mirror the behavior of long fibers in the lung.

The theory for calculating dissolution rate from biopersistence studies is described in the next section. The following section gives the results for 31 fibers obtained both from published and from previously unpublished biopersistence studies. The last section compares the in-vivo dissolution rate constant both with the in-vitro measured values for the fibers and with the weighted half times obtained from the biopersistence studies.

## THEORY AND METHODS

In what follows, the in-vitro dissolution rate will be extracted from two different types of animal studies, the long fiber retention data in inhalation biopersistence studies ([Bernstein et al., 1994](#)), and long fiber diameter data from intratracheal instillation studies ([Morgan et al., 1994](#)). The long fibers, or those longer than 20  $\mu\text{m}$  or too long to be enveloped effectively by the alveolar macrophage, are the ones thought to be most affected by dissolution, most likely because they spend the most time following inhalation in the extracellular environment of the lung. Therefore, the retention and diameter of these fibers longer than 20  $\mu\text{m}$  are the data used to obtain the dissolution rate in vivo.

Obtaining the in-vivo dissolution rate constant from the diameter of long fibers in intratracheal studies will be described first. In these studies, it was found that the decrease in the peak long fiber diameter, that is, the most probable diameter or the mode of the diameter distribution of fibers 20  $\mu\text{m}$  or longer, was predicted well by the in-vitro measured dissolution rate constant  $k_{dis}$  ([Eastes et al., 1995](#)). The observed diameter of a dissolving fiber at time  $t$  is given by

$$D(t) = D(0) - \frac{2k_{dis}t}{\rho} \quad \text{for } t \text{ such that } D(t) > D_{res} \quad (1)$$

and

$$D(t) = D_{res} \quad \text{otherwise,}$$

where  $D(t)$  is the diameter at time  $t$ ,  $\rho$  is the density of the fiber, and  $D(0)$  is the initial diameter of this fiber. One cannot expect to observe, much less to measure, the diameter of a fiber that is thinner than the limit of resolution  $D_{res}$  of the microscopic equipment. The value of  $D_{res}$  was taken to be 0.3  $\mu\text{m}$  for the light microscopic image analysis setup ([Eastes et al., 1995](#)).

In the case of fibers recovered from the animals' lungs at a given time, one does not know the initial diameter of each fiber needed in Eq (1), as the instilled fibers possess a range of diameters. However, the peak diameter, or the mode of the diameter distribution, will obey Eq (1), since all of the long fibers in the same extracellular environment are assumed in this model to dissolve at the same rate, differing only in their initial diameter.

It is most important to note that, while the peak diameter obeys Eq (1), the mean diameter, whether arithmetic or geometric mean or the median, does not. Even though all fibers decrease in diameter at the same rate as they dissolve in this model, the mean or median diameter may decrease, may remain approximately constant, or may even increase with time. This at first surprising result occurs because some fibers dissolve and are removed from the set of long fibers measured, while the remaining fibers decrease in diameter. Thus some fibers decrease in diameter, driving the average down, while others, the thinner ones initially, are eliminated, driving the average up. The average diameter is thus pulled in two directions during dissolution. The ultimate change in average diameter at any time is thus determined primarily by the initial distribution of diameters rather than by the dissolution rate. The result of these considerations is that the peak diameter is an appropriate statistic with which to follow long fiber diameter changes for the present purpose.

In order to obtain the in-vivo  $k_{dis}$ , the peak diameter of the long fibers recovered from the animals' lungs is fit to Eq (1) by minimizing the  $\chi^2$  statistic. The standard deviation of the peak diameter is also needed for this procedure. The pooled standard deviation of the peak diameter obtained from replicate measurements was found to be about 0.2  $\mu\text{m}$ , and this value was used for all measured peak diameters in the fit. There are two parameters determined by fitting the observed peak diameters to Eq (1), the in-vivo  $k_{dis}$  and the initial peak diameter  $D(0)$ .

Obtaining the in-vivo dissolution rate constant from the long fiber retention data in a short-term inhalation biopersistence study is similar in principle to that just described except that the model equation is different. The

model used here for the number of long fibers  $n(t)$  remaining at time  $t$  is

$$n(t) = n(0)[re^{-bt} + (1 - r)]f(k_{dis}, t). \quad (2)$$

This equation describes the retention of fibers  $20 \mu\text{m}$  or longer as two simultaneous processes, the short-term physiological clearance of a fraction  $r$  of the  $n(0)$  initially deposited fibers with a time constant  $b$ , and the dissolution of all the fibers with a dissolution rate  $k_{dis}$ . Given  $k_{dis}$  at time  $t$ , the fraction  $f(k_{dis}, t)$  of dissolving fibers remaining may be computed by applying Eq (1) to each fiber diameter  $D(0)$  in a large sample of long fibers measured at the initial sacrifice. The fraction of the long fibers initially present whose diameter is still as large or larger than  $D_{res}$  at time  $t$  is then  $f(k_{dis}, t)$ .

Two processes, short-term physiological clearance and dissolution, are included in Eq (2) because that appears to be the simplest model that can explain the observed long fiber retention. It has been observed that even long asbestos fibers, which are expected to dissolve very little over the entire lifetime of the rat, are partially cleared in several weeks after fiber inhalation ceases ([Hesterberg et al., 1998](#); [Musselman et al., 1994](#)). The mechanism by which the short-term clearance happens is probably a physiological clearance of those long fibers deposited in the ciliated airways, as opposed to those deposited in the alveolar spaces.

Although Eq (2) includes two major processes that govern long fiber retention, it is a substantial oversimplification of the real situation. One fact that this model does not comprehend is that a small number of long fibers remain in the animals' lungs at the longest sacrifice times even for moderately rapidly dissolving fibers, a phenomenon that may be observed in the data in nearly every biopersistence study ([Eastes and Hadley, 1995](#)). This minority of fibers may exist in macrogranulomas or in similar compartments in which the fibers do not dissolve as the majority do in the extracellular environment.

There are four independent parameters in the model of Eq (2), which are taken here to be  $k_{dis}$ ,  $n(0)$ ,  $r$ , and  $b$ . The first two, the in-vivo dissolution rate  $k_{dis}$  and the initial long fiber number  $n(0)$ , depend on the fiber type and on the test aerosol. But the short-term physiological clearing fraction  $r$  and its time constant  $b$  would be expected to be about the same for all fibers with a similar distribution of long fiber lengths and diameters, as was approximately the case in the studies used here. Under this assumption, the parameters  $r$  and  $b$  were determined by fitting the observed long fiber clearance curve of a fiber with an extremely low dissolution rate to Eq (2) with  $k_{dis}$  set to zero. When the dissolution rate is zero, then  $f(k_{dis}, t)$  is unity at all times  $t$ . The parameters for short-term physiological clearance  $r$  and  $b$  determined for this essentially non-dissolving fiber were then used for all other fibers. By this procedure, there were only two parameters,  $k_{dis}$  and  $n(0)$ , to be determined by fitting to the observed long fiber clearance of each test fiber. While the value of  $n(0)$  was fixed for each fiber to the average long fiber count at the first sacrifice time, leaving only one free parameter,  $k_{dis}$ , to be determined by the fit, all of the first sacrifice counts were included in the determination of  $\chi^2$

**Table 1.** Previously published biopersistence studies and the fibers tested in them.

Fibers	Study Type	Reference
7753, 7484, 7779, MMVF 10, MMVF 11	Intratracheal Instillation	<a href="#">Eastes et al., 1995</a>
Amosite, RCF 1a, Rock MMVF 21, E MMVF 32, JM475 MMVF 33, and HT MMVF 34	Short-term Inhalation	<a href="#">Hesterberg et al., 1998</a>
SG MMVF 11, SG A, SG B, SG C, SG F, SG G, SG H, SG J X607, and SG L	Short-term Inhalation	<a href="#">Bernstein et al., 1996</a>
Crocidolite, JM 901 MMVF 10, CT B MMVF 11, Rock Wool MMVF 21, and Slag Wool MMVF 22	Short-term Inhalation	<a href="#">Musselman et al., 1994</a>

The downhill simplex method of Nelder and Mead ([Press et al., 1992](#)) was used to fit both the inhalation and intratracheal studies. This method was used because it does not require that the derivatives of  $\chi^2$  with respect to the parameters be known or even exist. The absence of such derivatives is useful for these fits because Eq (1) has a discontinuous derivative at the point where  $D(t) = D_{res}$ , and Eq (2) has a factor  $f(k_{dis}, t)$  that is numerically determined for a discrete set of measured initial fiber diameters.

A measure of the uncertainty of the fitted parameters was determined in each case by the bootstrap method. The observed animal data were resampled 20 times and the best fit parameters were tabulated for each such data set. These lists of parameters obtained from resampled data sets were used to obtain statistics such as the geometric standard deviation of the in-vivo dissolution rate.

The method just described was applied to all of the biopersistence studies for which the data have been reported or are available in sufficient detail to perform the calculations. Many of the inhalation biopersistence studies used to obtain the results described here have been published previously and are summarized in Table 1. In a few cases, essentially the same fiber composition was tested more than once, and the names used to distinguish the fibers reflect that fact. The conventional rock wool MMVF 21 appears in two studies and the (borosilicate) glass wool MMVF 11 appears in three. The glass wool MMVF 10 was tested once by inhalation biopersistence and once by intratracheal instillation. Both crocidolite and amosite asbestos were tested in separate inhalation biopersistence studies. The borosilicate glass wool fibers in this set range from the slowly dissolving 7779, through rapidly dissolving 7753, 7484, MMVF 10, and MMVF 11, to very rapidly dissolving SG A, SG B, and SG C. The rock and slag wool fibers also exhibited this range of dissolution rates from the slowly dissolving MMVF 21 and SG L to rapidly clearing low-alumina SG F, SG G, and SG H, to rapidly clearing high-alumina HT MMVF 34. Two fibers with compositions differing from all of these just mentioned are the slowly dissolving refractory ceramic fiber RCF 1a and a thin fiber E glass, E MMVF 32. Also included in the set is a rapidly dissolving calcium silicate composition SG J X607.

**Table 2.** Weight percent oxide composition of fibers in previously unpublished inhalation biopersistence studies.

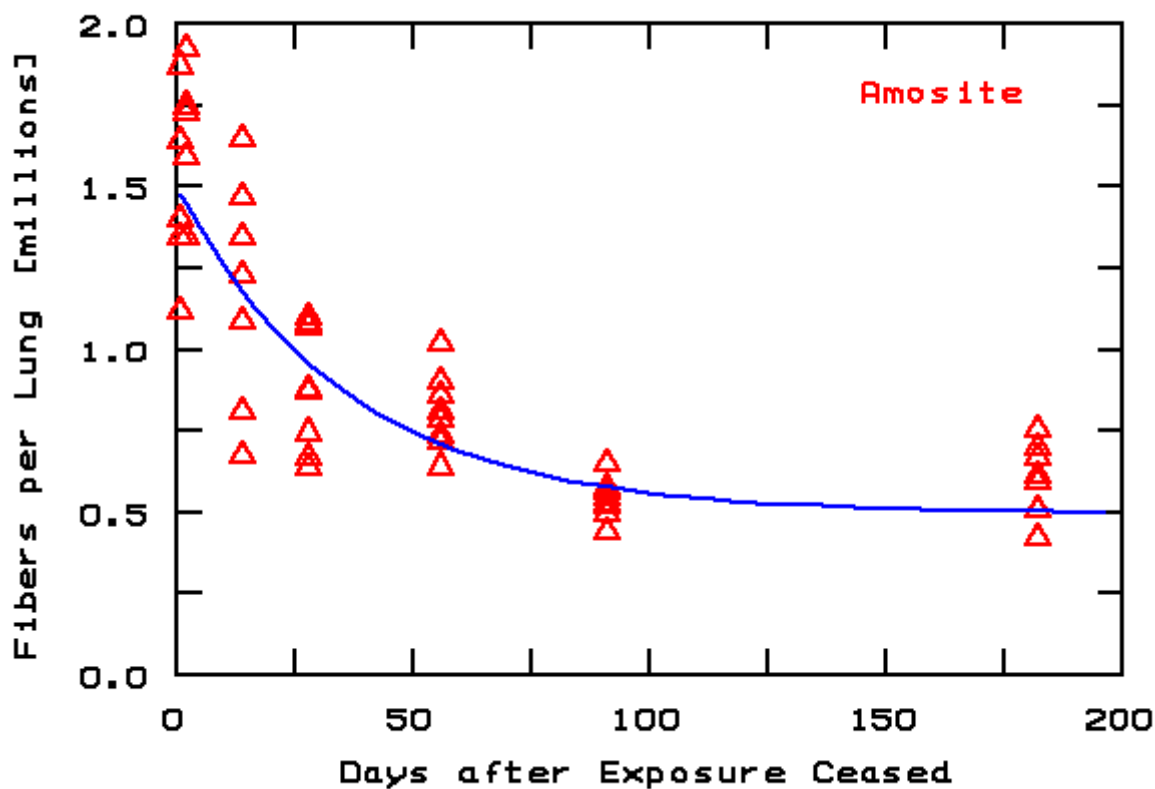
Oxide	QFHA 19	QFHA 22	QFHA 23	QFHA 25	NK 8340	KI-40
SiO <sub>2</sub>	40.14	41.62	39.53	38.26	64.92	54.06
Al <sub>2</sub> O <sub>3</sub>	18.91	21.62	21.92	22.73	2.12	2.05
Na <sub>2</sub> O	1.77	1.72	1.94	0.74	14.56	17.17
K <sub>2</sub> O	0.45	0.43	0.43	0.39	0.51	0.83
B <sub>2</sub> O <sub>3</sub>	-	-	-	-	4.66	15.66
CaO	19.12	15.56	16.76	25.19	9.08	7.50
MgO	11.57	9.83	11.01	6.58	3.03	1.80
Fe <sub>2</sub> O <sub>3</sub> <sup>a</sup>	5.94	7.31	6.86	4.40	0.50	0.136
FeO	4.62	5.54	4.95	3.38	0.12	0.056
TiO <sub>2</sub>	1.58	1.65	1.64	1.17	0.05	0.082

<sup>a</sup>Total iron reported as Fe<sub>2</sub>O<sub>3</sub>

The remaining six fibers were studied by inhalation biopersistence but have not been published previously. The compositions of these fibers are given in Table 2 in oxide weight percent. Those studies were carried out at the Research and Consulting Company (RCC) in Switzerland with the fiber counting and measurement done at GSA in Germany. The short-term inhalation biopersistence protocol used there was virtually identical to that of the other studies ([Bernstein et al., 1994](#)). The fibers labeled QFHA are high-alumina rock wool compositions with an alumina content roughly indicated by the trailing digits. NK 8340 is a conventional borosilicate glass wool fiber and KI-40 is a fiber with a "Carcinogenicity Index"  $K_I$  above 40 ([BMA, 1995](#)).

## RESULTS

The in-vivo dissolution rate constant  $k_{dis}$  determined from fitting the long fiber diameter changes following intratracheal instillation to the model Eq (1) are shown in Table 3. In Table 3 and in the next two tables, a number of statistics of the fit are shown. The standard error of the parameter determined by the fit is shown only for  $k_{dis}$  since that is the parameter of greatest interest. It is expressed as the geometric standard error and may be interpreted in the following way: If the best fit  $k_{dis}$  is 100 and the geometric standard error is 2, then approximately two-thirds of the values are expected to lie between  $100/2$  and  $100 \times 2$  or between 50 and 200. The statistic  $R^2$  is the fraction of the variance of the data that is accounted for by the prediction. The significance of the  $\chi^2$  statistic  $P$  is the probability that the extent to which the measured data deviate from the model are consistent with random variations with the estimated standard error.



L

**Figure 1.** Observed long fiber retention data (red triangles) for Amosite asbestos compared with the fit to the model (solid blue curve) with a zero dissolution rate constant. The parameters for short-term physiological clearance determined for this essentially non-dissolving fiber were used for all other fibers.

In order to determine the in-vivo dissolution rate constant from the inhalation biopersistence studies, the parameters of the short-term physiological clearance, which are assumed to be the same for all of these fibers of

similar length and diameter distribution, must be obtained. These parameters were determined by fitting the model Eq (2) with  $k_{dis} = 0$  to the observed long fiber clearance results for Amosite asbestos. This fiber was chosen for this purpose because it has been found to have a very small dissolution rate in vitro and a long biopersistence, and because the length and diameter distribution of this sample was similar to that of the other fibers considered here. Another possibility would be the Crocidolite asbestos fiber tested in an earlier biopersistence study, but it had a significantly different length and diameter distribution from the other synthetic vitreous fibers, and there were only a few long fibers in the lungs at every sacrifice time. The best fit short-term physiological clearance parameters for Amosite were found to be  $r = 0.663$  and  $b = 0.0280$ , which are parameters in Eq (2). These values indicate that 66% of the inhaled long fibers are subject to short-term physiological clearance with a time constant  $b$  corresponding to a half life of about 25 days. The  $R^2$  statistic for the fit was 0.779 and the significance of  $\chi^2$  was 0.030, indicating that the model explains the observed long fiber clearance well and reasonably within the variation of the animal data themselves. The long fiber retention data (red triangles) and the model fit (solid blue curve) for this fiber are shown in Figure 1.

**Table 3.** In-vivo dissolution rate constants  $k_{dis}$  in ng/cm<sup>2</sup>/hr and statistics determined from long fiber diameter changes in intratracheal instillation studies.

Fiber	$k_{dis}$	gsd <sup>a</sup>	$R^2$	$P^b$	$N^c$
7753	244	1.309	0.880	0.204	12
7484	124	1.227	0.832	0.021	7
7779	3	2.614	0.245	0.965	15
MMVF 10	201	1.316	0.819	0.399	4
MMVF 11	96	1.170	0.736	0.334	6

<sup>a</sup>Geometric standard deviation of  $k_{dis}$

<sup>b</sup>Significance of  $\chi^2$

<sup>c</sup>Number of data, in this case sacrifice times

With the parameters  $r$  and  $b$  in Eq (2) determined from Amosite, the model was fit to the other fibers in these studies to obtain in-vivo dissolution rates for each. The results and statistics of the fit are summarized in Table 4 for the previously unpublished biopersistence studies and in Table 5 for the previously published ones.

**Table 4.** In-vivo dissolution rate constants  $k_{dis}$  in ng/cm<sup>2</sup>/hr and other parameters and statistics determined from long fiber retention in previously unpublished short-term inhalation biopersistence studies.

Fiber	$k_{dis}$	gsd <sup>a</sup>	$R^2$	$P^b$	$N^c$
QFHA 19	974	1.057	0.779	0.000	58
QFHA 22	406	1.278	0.704	0.000	58
QFHA 23	495	1.183	0.841	0.083	58
QFHA 25	337	1.110	0.611	0.819	57
NK 8340	445	1.251	0.794	0.000	58
KI-40	1198	2.923	0.520	0.998	58

<sup>a</sup>Geometric standard deviation of in-vivo  $k_{dis}$

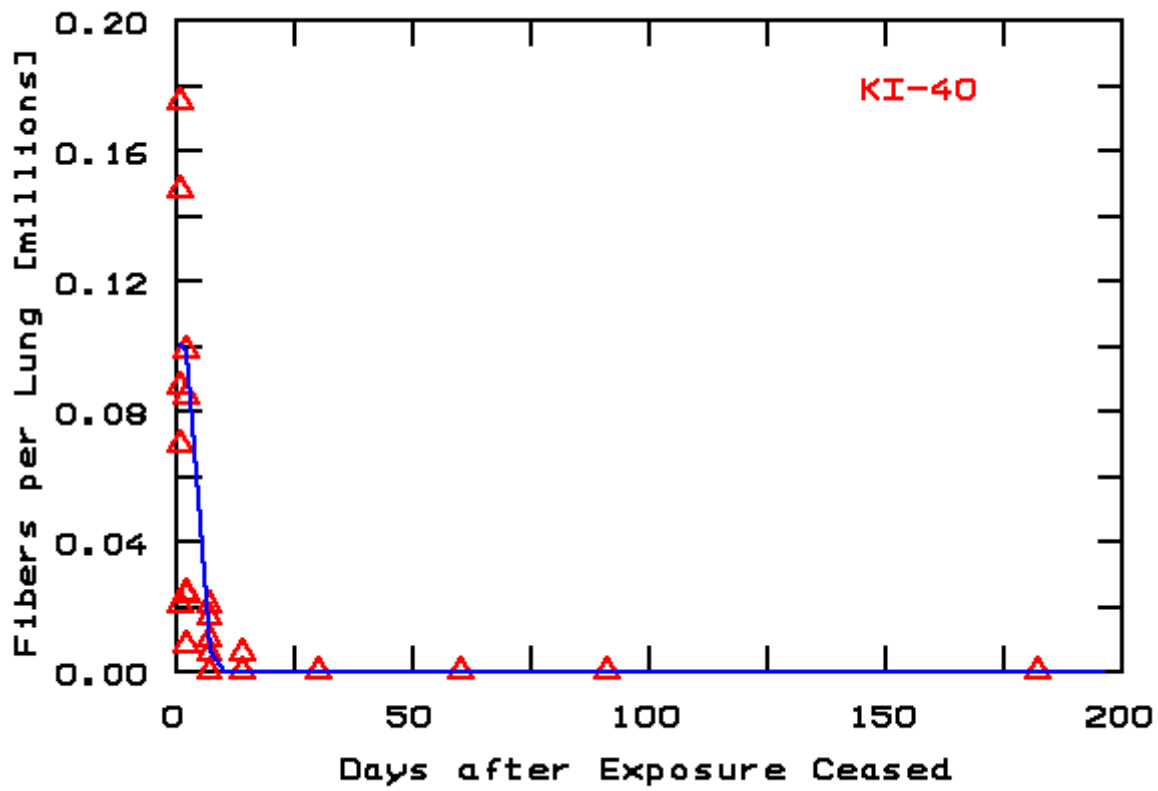
<sup>b</sup>Significance of  $\chi^2$

<sup>c</sup>Number of data, in this case animals involved

**Table 5.** In-vivo dissolution rate constants  $k_{dis}$  in ng/cm<sup>2</sup>/hr and other parameters and statistics determined from long fiber retention in previously published short-term inhalation biopersistence studies. The footnotes refer to Table 4.

Fiber	$k_{dis}$	gsd <sup>a</sup>	$R^2$	$P^b$	$N^c$
Amosite	8	2.615	0.781	0.054	58
RCF 1a	16	1.078	0.773	0.000	58
Rock MMVF 21	20	1.022	0.834	0.002	58
E MMVF 32	11	1.028	0.709	0.000	58
JM475 MMVF 33	17	2.549	0.373	0.000	58
HT MMVF 34	346	1.068	0.948	0.000	58
SG MMVF 11	138	1.512	0.648	0.101	25
SG A	225	1.514	0.351	0.000	25
SG B	989	4.655	0.463	0.331	20
SG C	616	2.024	0.612	0.868	25
SG F	180	1.331	0.701	0.786	25
SG G	175	1.347	0.809	0.595	25
SG H	126	1.649	0.750	0.000	25
SG J X607	222	1.718	0.770	0.000	25
SG L	26	1.974	0.427	0.111	25
Crocidolite	2	10.485	0.036	0.043	38
JM 901 MMVF 10	36	1.419	0.659	0.462	26
CT B MMVF 11	133	1.245	0.794	0.000	27
Rock Wool MMVF 21	25	1.042	0.823	0.052	26
Slag Wool MMVF 22	171	1.563	0.597	0.012	27

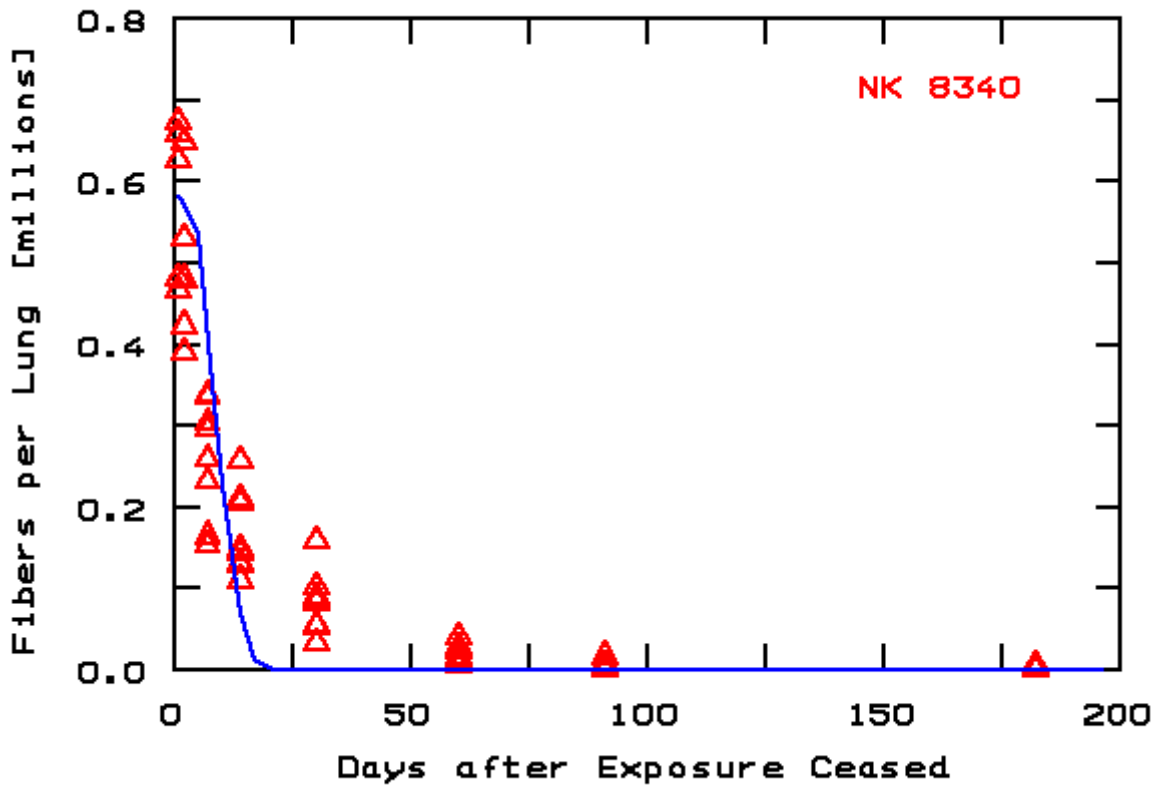
Although the statistics in Tables 4 and 5 summarize the fit, it is still useful to compare the long fiber retention data with the values calculated from the model for the best fit parameters given in Tables 4 and 5. Figure 2 shows this comparison for the fiber type KI-40, which is typical of those for which the model fit the data within the variations in the data themselves, as evidenced by significance values  $P$  well above 0.001. Figures 3 and 4 show typical examples of the fiber types for which the significance was less than 0.001, indicating that the model was not able to fit the data to within the variations in the data themselves.



L

**Figure 2.** Long fiber retention in individual animals ( red triangles) for fiber type KI-40, a very rapidly dissolving fiber, compared to the model (solid blue curve).





L

**Figure 4.** Long fiber retention in individual animals (red triangles) for the borosilicate glass fiber NK 8340 compared to the model (solid blue curve). The model fails here to reproduce the observed long fiber lung burden at one month, whereas it passes through the data at the other sacrifice times.

It is useful to express the dissolution rate in terms of the fiber dissolution time  $t_{dis}$  (Eastes et al., 2000) and to compare it to the weighted  $T_{half}$  for long fiber clearance, (Maxim et al., 1999; Bernstein et al., 1997). These quantities for the previously unpublished inhalation biopersistence studies are given in Table 6. The fiber dissolution time  $t_{dis}$  in units of days/ $\mu\text{m}$  is the time required to dissolve a  $1\ \mu\text{m}$  fiber and is related to  $k_{dis}$  by

$$t_{dis} = \frac{\rho}{2k_{dis}}, \quad (3)$$

where  $\rho$  is the density of the fiber, also given for these fibers in Table 6. The weighted  $T_{half}$  is a weighted sum of the short and long term clearance described by the following model (Bernstein et al., 1997):

$$n(t) = a_1 e^{-b_1 t} + a_2 e^{-b_2 t} \quad (4)$$

The weighted  $T_{half}$  in Table 3 is the average of the  $T_{half}$  values corresponding to  $b_1$  and  $b_2$  weighted by  $a_1$  and  $a_2$ . It is seen by comparing Eq (4) with (2) that both have the same form for short-term clearance, but Eq (4) treats the other component as a separate form of physiological clearance, whereas Eq (2) superimposes a model of fiber dissolution on both components.

**Table 6.** Weighted  $T_{half}$  for long fiber clearance in inhalation biopersistence studies compared with in-vivo  $t_{dis}$  obtained from the same studies, both in days, in order of increasing  $t_{dis}$ .

Fiber	wt. $T_{half}$	$t_{dis}$	gsd <sup>a</sup>	$\rho^b$
KI-40	1.3	4.5	2.923	2.6

QFHA 19	4.5	6.1	1.057	2.83
NK 8340	8.8	11.9	1.251	2.55
QFHA 23	5.5	11.9	1.183	2.82
QFHA 22	5.9	14.5	1.278	2.82
QFHA 25	7.9	17.5	1.110	2.83

<sup>a</sup>Geometric standard deviation of  $t_{dis}$

<sup>b</sup>Fiber density in  $\text{g/cm}^3$

## DISCUSSION

It is clear from the statistics of the fits in Tables 3 through 5 that the models chosen agree with the animal data reasonably well and provide an in-vitro dissolution rate constant  $k_{dis}$  that describes the long fiber behavior in vivo. The majority of the fits have values of  $R^2$  above 70% indicating that the model explains over 70% of the variation in the experimental data. The two fiber types for which the  $R^2$  statistic was low were 7779 from intratracheal instillation and Crocidolite from an inhalation study. In both cases,  $R^2$  was low because the fibers dissolved so slowly that there was little change over the time of the study. Additionally, in the case of Crocidolite, there were few long fibers initially. In these cases, low  $R^2$  does not indicate a poor fit. In fact, the model fit the data reasonably well, and the small dissolution rates found reflect that lack of dissolution.

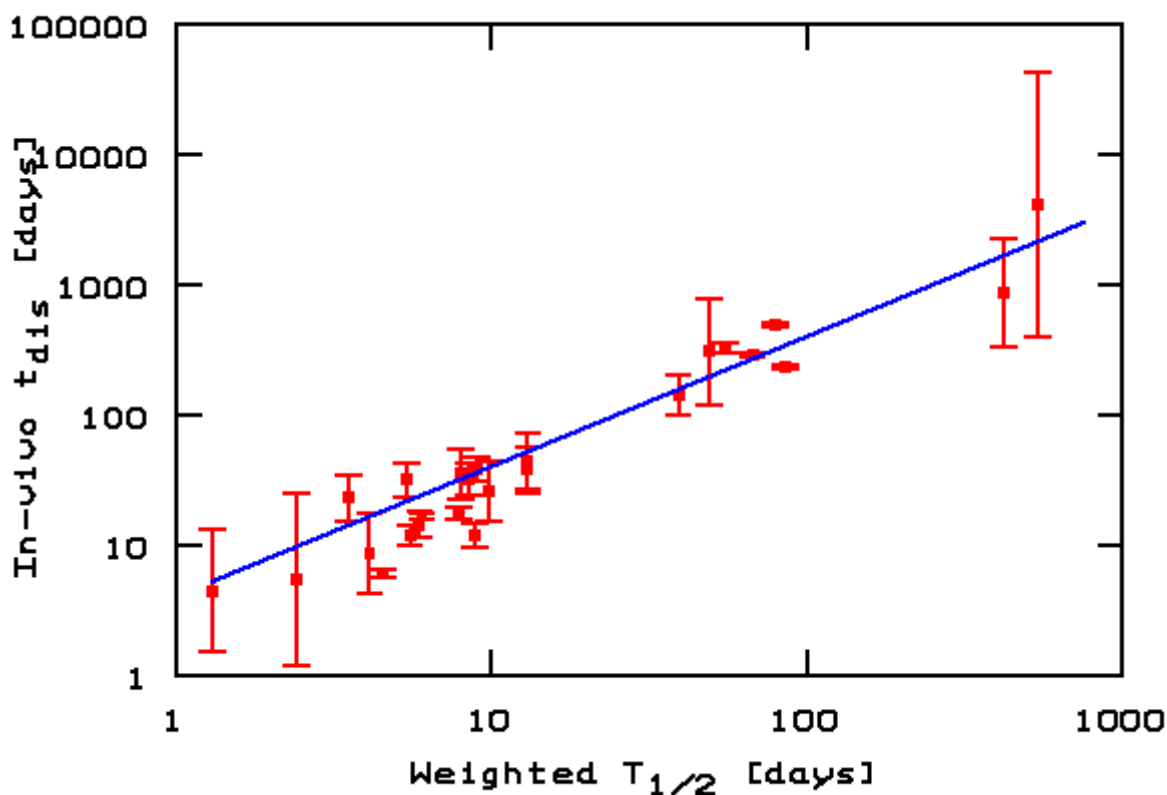
Another measure of the quality of fit of a model is the significance  $P$  of the  $\chi^2$  statistic, which is the probability that the observed deviations of the experimental data from the model could have arisen by chance in data with the standard deviation estimated. A rule of thumb often used ([Press et al., 1992](#)) is that  $P < 0.001$  indicates that there are at least some features of the data that the model fails to reproduce that are unlikely to be merely random variations. Such a low value of the significance does not necessarily indicate that the model is useless, but merely that there are some features in the data that are not explained by the model. Even when the significance is low, the model may still be useful for estimating the dissolution rate in vivo, since the  $R^2$  statistic indicates that the model is capturing a significant part of the behavior of long fiber clearance.

The reasonably large values of the significance  $P$  in Table 3 show that the model for long fiber diameter change in the lung following intratracheal instillation explains the data to within the estimated variations in the data. The same conclusion holds for about 60% of the fibers in Tables 4 and 5 from the inhalation biopersistence studies. On the other hand, the other 40% of the fibers studied by inhalation biopersistence have significance values less than 0.001, indicating features of the data not captured by the model Eq (2). Two typical examples of these fibers are shown in Figures 3 and 4. Sometimes the low significance of the fit is caused by fiber counts at one sacrifice time that fail to decrease or even increase relative to the trend of the previous sacrifices, in an apparently anomalous way. In most of these cases,  $R^2$  is reasonably large, suggesting that the model reflects much of the long fiber clearance behavior, but not all.

Another factor contributing to the number of results with low significance values is the simplicity of the model. Aside from the initial long fiber count, the only adjustable parameter for the fit is the in-vivo dissolution rate constant  $k_{dis}$ . The other two short term parameters have been fixed independently by the Amosite fiber data. The quality of the fit is vastly improved in all cases if all four parameters are allowed to vary independently for each fiber. In fact, the model of Eq (4) that is used to define the weighted  $T_{half}$  has just such four parameters that are varied independently for each fiber. But for the present dissolution model of Eq (2), there is no known biological justification for different short term physiological clearance for different fibers that have roughly the same length and diameter distributions, and thus such results are not presented here.

An interesting feature of the model Eq (2) for long fiber clearance in an inhalation biopersistence study is that, whereas only a fraction  $r$  participate in short-term physiological clearance with time constant  $b$ , all long fibers are considered to dissolve at the given dissolution rate. Another alternative would be to allow only the fraction  $1-r$  of fibers, or 34% in this case, that do not participate in short-term physiological clearance to dissolve by moving the brackets in Eq (2). That this alternative model cannot be correct may be seen by comparing Figure 1 for Amosite that does not dissolve with Figure 2 for a very rapidly dissolving fiber KI-40. These figures were drawn to the same time scale to facilitate this comparison. If dissolution affected only the 34% portion of fibers, then it would be impossible for the model curve to approach zero in much less than the 75 days needed for it to level off in Figure 1. Certainly the model would not approach zero long fibers in the 10 days or so seen in Figure 2. These considerations indicate that all of the long fibers, both the fraction that participate in short-term physiological clearance and those that do not, are involved in dissolution. This result appears reasonable given that both sets of long fibers are expected to reside primarily in the extracellular environment.

The comparison of the in-vivo dissolution time  $t_{dis}$  with the weighted  $T_{half}$  derived from Eq (4) is instructive also. The in-vivo  $t_{dis}$  corresponding to the in-vivo  $k_{dis}$  in Tables 4 and 5 are plotted in Figure 5 against the weighted  $T_{half}$  from Table 6 for the previously unpublished studies and from the published weighted  $T_{half}$  for the other fiber types. That  $t_{dis}$  and weighted  $T_{half}$  are not the same is expected from the different equations upon which they are based. That they correlate reasonably well is expected, since the main property that leads to different values of weighted  $T_{half}$  for different fiber types is the different dissolution rates, which are expressed by  $t_{dis}$ . Compared to the weighted  $T_{half}$ , the parameter  $t_{dis}$  is seen to be a way of expressing the difference between fibers in terms of the actual process that distinguishes them, that is, dissolution, without coupling the effects of other clearance mechanisms that appear to act the same for all fibers that have the same length and diameter distribution.



L

**Figure 5.** Weighted  $T_{half}$  for short-term inhalation biopersistence studies of a series of fibers compared to the in-vivo fiber dissolution time  $t_{dis}$ , which is inversely related to its dissolution rate constant  $k_{dis}$ . The vertical red

bars show the geometric standard deviation of the in-vivo  $t_{dis}$ . The data displayed in this figure along with other information about the same fibers are available separately as a tab delimited text file by [clicking here](#).

The good correspondence between in-vivo  $t_{dis}$  and weighted  $T_{half}$  shown in Figure 5 leads one to expect that one would be a good predictor of the other, and such is the case. The  $R^2$  statistic for the correlation of  $t_{dis}$  with weighted  $T_{half}$  is 0.786, meaning that nearly 79% of the variation in weighted  $T_{half}$  is explained by  $t_{dis}$ . Since one would expect the weighted  $T_{half}$  to approach zero when  $t_{dis}$  does, one is led to express  $t_{dis}$  as a multiple of weighted  $T_{half}$  in this way:

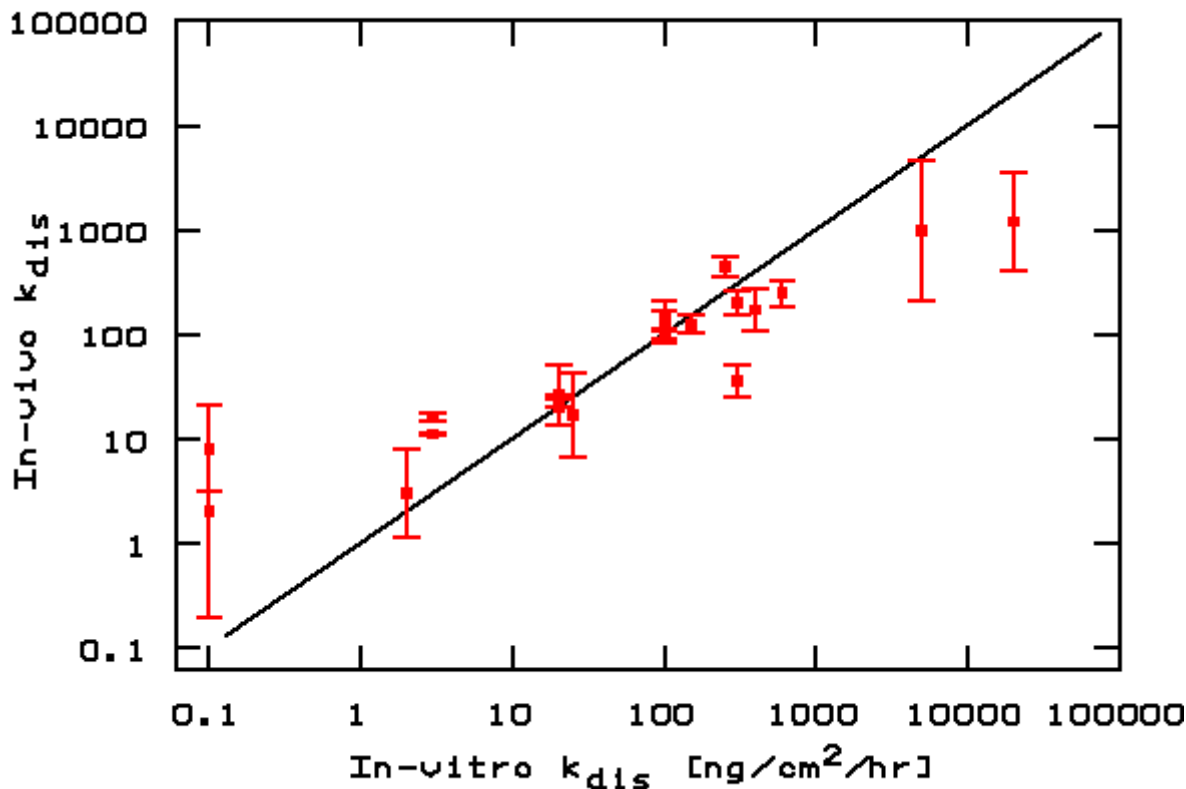
$$t_{dis} = BT_{\frac{1}{2}} \quad \text{where} \quad B = 4.068 \quad x/1.014. \quad (5)$$

The value of the multiplier  $B$  was obtained by fitting the logarithmic data of Figure 5 to Eq (5), and the best fit line is shown in Figure 5. The standard error of  $B$  is expressed as a factor in Eq (5) because it is derived from the geometric standard error that appears naturally when using logarithmic data. It is seen from Eq (5) that in-vivo  $t_{dis}$  is about four times the weighted  $T_{half}$ . It is this much larger because  $t_{dis}$  includes only dissolution, whereas weighted  $T_{half}$  is influenced by the short term physiological clearance that appears unrelated to dissolution.

An important result of Figure 5 and Eq (5) is that the 10 day weighted  $T_{half}$  required for exoneration of a fiber from classification by Note Q of the European Commission Directive 97/69/EC ([EC, 1997](#)) corresponds to a dissolution time of about 40 days/ $\mu\text{m}$  or a dissolution rate  $k_{dis}$  of about 120 ng/cm<sup>2</sup>/hr. Thus the in-vivo dissolution rate required to exonerate a fiber with an inhalation biopersistence test under the EC Directive is greater, although not significantly so, than that predicted to avoid fibrosis in a chronic inhalation test ([Eastes and Hadley, 1996](#)).

There is good correlation ( $R^2 = 0.727$ ) and also reasonably good agreement between the in-vivo  $k_{dis}$  and the  $k_{dis}$  as measured in vitro for the same fibers, which may be seen in Figure 6 in which these data are plotted. There seems to be a trend in Figure 6 for the in-vivo  $k_{dis}$  to be somewhat smaller than what is measured in vitro for the largest values of  $k_{dis}$ , and just the reverse at the smallest  $k_{dis}$  values. These effects are probably significant, although the geometric standard error of the in-vivo  $k_{dis}$  is large in many of these cases. The most likely explanation for this observation is that the precision of the in-vivo measurement is best in the range of 3 to 300 ng/cm<sup>2</sup>/hr but becomes increasingly poor as the dissolution rate moves outside that range. At low dissolution rates, there is so little clearance of long fibers (other than the short-term physiological clearance) within the time span of the study that small variations in the data are computed by this method as some small value of a dissolution rate. The values of  $k_{dis}$  between 1 and 10 ng/cm<sup>2</sup>/hr obtained by fitting a non-zero  $k_{dis}$  to the Amosite and Crocidolite asbestos reported in Table 5 are therefore not to be taken literally, but could be several orders of magnitude below these values and still be consistent with the experimental data. On the other hand, the large in-vivo dissolution rates are not accurately indicated either, because nearly all the long fibers are gone by the first few sacrifice times in the protocol used here, as seen in Figure 2, for example. As indicated by the large geometric standard error, the in-vivo dissolution rate could be much larger and still be consistent with these animal data.

There is one significant deviation that deserves comment, the fiber MMVF 10 with an in-vitro  $k_{dis}$  of 200, significantly below the line in Figure 6. This fiber type was tested twice in vivo, once by intratracheal instillation yielding an in-vivo  $k_{dis}$  agreeing well with in-vitro (Table 3), and again by inhalation yielding a  $k_{dis}$  of 36 ng/cm<sup>2</sup>/hr (Table 5). It is this latter point that appears significantly out of place in Figure 6. There is no apparent explanation for this discrepancy, especially as another glass wool, MMVF 11, with an in-vitro  $k_{dis}$  of 100, was tested three times with in-vivo values ranging from 96 to 138. Still another fiber, the conventional rock wool MMVF 21, was also tested three times, if one includes the similar composition SG L, with an in-vivo  $k_{dis}$  ranging from 20 to 26 compared to 20 in vitro for MMVF 21. Except for this one MMVF 10 result, the in-vivo dissolution rate constants are remarkably consistent with one another and with in-vitro measurements.



L

**Figure 6.** In-vivo  $k_{dis}$  determined from inhalation and intratracheal biopersistence studies compared to the in-vitro measured  $k_{dis}$  for the same fiber compositions. The data displayed in this figure along with other information about the same fibers are available separately as a tab delimited text file by [clicking here](#).

A more serious discrepancy between the in-vivo and the in-vitro  $k_{dis}$  lies in the inability to measure the dissolution rate of certain high-alumina fibers by the in-vitro protocol. No values are plotted in Figure 6 for in-vitro  $k_{dis}$  of these fibers because the conditions of the protocol ([Bauer et al., 1997](#)) are not met and, by that protocol, no in-vitro  $k_{dis}$  can be determined unambiguously. The conditions of the protocol are not met in the sense that the measured dissolution rate continues to rise as the solution flow rate is increased, making it difficult to determine a limiting value, or whether one even exists. The difficulty may be related to the presence of significant amounts of aluminum that have dissolved from the fibers into the solution. It is known that even very small amounts of aluminum (and to a lesser extent silicon) in solution slow the dissolution rate significantly ([Mattson, 1995](#)). It may be that there is some mechanism in the lung that removes aluminum from the lung fluid in a way that is not simulated in vitro. This matter is the subject of on-going research. In any case, the methods described in this paper provide a way to obtain a dissolution rate for such fibers.

There is a body of excellent scientific work that models the deposition and retention of particles in the lungs (Stöber, 1999, and references cited therein), but these usually do not treat dissolution as a physical chemical process. One such attempt ([Yu et al., 1998](#)) made two separate errors in estimating the dissolution rate. The first error was to estimate the dissolution rate from the decrease in the geometric mean diameter, a statistic that is not related to dissolution rate, as discussed previously. The second error was to use the mean diameter of all fibers, not just the long ones. Since the majority of fibers in the lung are shorter than 20  $\mu\text{m}$  and do not participate in extracellular dissolution by the same mechanism, it is clear that these are not likely to dissolve nor to decrease in diameter with time by the same kinetics. Both of these errors, each of which tend to underestimate the dissolution rate significantly, led to estimated dissolution rates that were about 1% of what occurs in vivo as shown in the current paper. Since dissolution was estimated to be much smaller than the value obtained either in vitro or in the present work, another mechanism was needed to explain the observed fiber clearance. Fiber

breakage was postulated as this separate mechanism. There is no question that long fibers that dissolve must eventually break. If this inevitable breakage occurs late in the life of the long fiber as a result of extensive dissolution, then it need not be accounted for as a separate mechanism. It is then included in dissolution. The present work, which treats dissolution as a physical chemical process, does not require any additional breakage mechanism to adequately explain the observed long fiber clearance.

The understanding of the critical role of long fiber dissolution in moderating the biological effects of synthetic vitreous fibers has developed rapidly over the last decade. Fibers shown not to be biopersistent by various in-vivo tests are now exonerated from classification as possible carcinogens by the EC Directive ([EC, 1997](#)). It is known that the dissolution and removal of long fibers is controlled predominately by physical chemical rather than by biological processes. Further elucidation of the relationships between fiber composition and long fiber dissolution and removal from the lung offers the potential for the eventual design and control of fiber dissolution rates absent the requirement for extensive animal testing. It is hoped that the present work contributes to that understanding.

## ACKNOWLEDGMENTS

The authors are grateful to their colleagues Dr. A. Dotti and Dr. Ph. Thévenaz at RCC for supervising the inhalation biopersistence studies and to Dr. U. Teichert at GSA for managing the fiber measurements. Without their expert help to insure accurate and reproducible technique in most of the studies used in this paper, the interpretation of these studies in terms of more fundamental quantities like dissolution rate would not have been possible.

## REFERENCES

- Bauer, J., Mattson, S. M., and Eastes W. 1997. In-vitro acellular method for determining fiber durability in simulated lung fluid. Available from the authors.  
[Read this paper](#) or [Download it](#) (24 kB).
- Bernstein, D. M., Morscheidt, C., de Meringo, A., Schumm, M., Grimm, H. G., Teichert, U., Thévenaz, P., Mellon, L. 1997. The biopersistence of fibres following inhalation and intratracheal instillation exposure. *Ann. occup. Hyg.* 41(Suppl. 1):224-230.
- Bernstein, D. M., Morscheidt, C., Grimm, H.-G., Thévenaz, P., and Teichert, U. 1996. Evaluation of soluble fibers using the inhalation biopersistence model, a nine-fiber comparison. *Inhal. Toxicol.* 8:345-385.
- Bernstein, D. B., Mast, R., Anderson, R., Hesterberg, T. W., Musselman, R., Kamstrup, O.; Hadley, J. 1994. An experimental approach to the evaluation of the biopersistence of respirable synthetic fibers and minerals *Environ. Health Perspect.* 102(Suppl. 5):15-18.
- BMA. 1995. Neufassung TRGS 905. *Bundesarbeitsblatt* 4/1995, pp. 70-71.
- Eastes, W., Potter, R. M., and Hadley, J. G. 2000. Estimating in-vitro glass fiber dissolution rate from composition. *Inhal. Toxicol.* 12:269-280.  
[Read this paper](#) or [Download it](#) (23 kB).
- Eastes, W., and Hadley, J. G. 1996. A mathematical model of fiber carcinogenicity and fibrosis in inhalation and intraperitoneal experiments in rats. *Inhal. Toxicol.* 8:323-343.  
[Read this paper](#) or [Download it](#) (60 kB).
- Eastes, W., Morris, K. J., Morgan, A., Launder, K. A., Collier, C. G., Davis, J. A., Mattson, S. M., and Hadley, J. G. 1995. Dissolution of glass fibers in the rat lung following intratracheal instillation. *Inhal. Toxicol.* 7:197-213.  
[Read this paper](#) or [Download it](#) (57 kB).
- Eastes, W., and Hadley, J. G. 1995. Dissolution of fibers inhaled by rats. *Inhal. Toxicol.* 7:179-196.

- Eastes, W. and Hadley, J. G. 1994. Role of fiber dissolution in biological activity in rats. *Regul. Toxicol. Pharmacol.* 20:S104-S112.
- EC, 1997. European Commission Directive 97/69/EC. *Official Journal of the European Communities* L343:19-20.
- Hesterberg, T. W., Chase, G., Axten, C., Miiller, W. C., Musselman, R. P., Kamstrup, O., Hadley, J., Morscheidt, C., Bernstein, D. M., Thévenaz, P. 1998. Biopersistence of synthetic vitreous fibers and amosite asbestos in the rat lung following inhalation. *Toxicol. and Applied Pharm.* 151:262-275.
- Knudsen, T., Guldborg, M., Christensen, V. R., Jensen, S. L. 1996. A new type of stonewool (HT fibres) with a high dissolution rate at pH = 4.5. *Glastech. Ber. Glass Sci. Technol.* 69:331-337.
- Mattson, S. 1994. Glass fibers in simulated lung fluid: Dissolution behavior and analytical requirements. *Ann. occup. Hyg.* 38:857-877.  
[Read this paper](#) or [Download it](#) (57 kB).
- Mattson, S. 1995. Factors affecting fiber dissolution -- in-vitro experiments. Presented at XVII International Congress on Glass, Beijing, China. Available from the authors.
- Maxim, D. L., Mast, R. W., Utell, M. J., Yu, C. P., Boymel, P. M., Zoitos, B. K., Cason, J. E. 1999. *Regul. Toxicol. Pharmacol.* 30:54-74.
- Morgan, A., Morris, K. J., Launder, K. A., Hornby, S. B., Collier, C. G. 1994. Retention of glass fibres in the rat trachea following administration by intratracheal instillation. *Inhal. Toxicol.* 6:241-251.
- Musselman, R. P., Miiller, W. C., Eastes, W., Hadley, J. G., Kamstrup, O., Thévenaz, P., Hesterberg, T. W. 1994. Biopersistences of man-made vitreous fibers and crocidolite fibers in rat lungs following short-term exposures *Environ. Health Perspect.* 102(Suppl. 5):139-143.
- Potter, R. M. and Mattson, S. M. 1991. Glass fiber dissolution in a physiological saline solution. *Glastech. Ber.* 64:16-28.
- Press, W. H., Teukolsky, S. A., Vetterling, W. T. and Flannery, B. P., 1992. *Numerical Recipes in C.*, 2nd ed., Ch. 10, pp. 408-412 and Ch. 15, pp. 656-661. New York: Cambridge University Press.
- Scholze, H. 1988. Durability investigations on siliceous man-made mineral fibers, a critical review. *Glastech. Ber.* 61:161-171.
- Stöber, W. 1999. POCK model simulations of pulmonary quartz dust retention data in extended inhalation exposures of rats. *Inhal. Toxicol.* 11:269-292.
- Yu, C. P., Dai, Y. T., Boymel, P. M., Zoitos, B. K., Oberdömlinger, G., Utell, M. J. 1998. A clearance model of man-made vitreous fibers (MMVFs) in the rat lung. *Inhal. Toxicol.* 10:253-274.

---

[First Page](#) || [Next Page](#)